K^+ Occupancy of the *N*-methyl-D-aspartate Receptor Channel Probed by Mg^{2+} Block

Yongling Zhu and Anthony Auerbach

From the Department of Physiology and Biophysics, State University of New York at Buffalo, Buffalo, New York 14214

ABSTRACT The single-channel kinetics of extracellular Mg^{2+} block was used to probe K^+ binding sites in the permeation pathway of rat recombinant NR1/NR2B NMDA receptor channels. K^+ binds to three sites: two that are external and one that is internal to the site of Mg^{2+} block. The internal site is ~0.84 through the electric field from the extracellular surface. The equilibrium dissociation constant for this site for K^+ is 304 mM at 0 mV and with Mg^{2+} in the pore. The occupancy of any one of the three sites by K^+ effectively prevents the association of extracellular Mg^{2+}. Occupancy of the internal site also prevents Mg^{2+} permeation and increases (by approximately sevenfold) the rate constant for Mg^{2+} dissociation back to the extracellular solution. Under physiological intracellular ionic conditions and at −60 mV, there is ~1,400-fold apparent decrease in the affinity of the channel for extracellular Mg^{2+} and ~2-fold enhancement of the apparent voltage dependence of Mg^{2+} block caused by the voltage dependence of K^+ occupancy of the external and internal sites.

KEY WORDS: ion binding sites • magnesium • channel block • permeation • selectivity

INTRODUCTION

The *N*-methyl-D-aspartate receptor (NMDAR)[1] channel is permeable to Na^+, K^+, and Ca^{2+}, and is blocked by Zn^{2+} and Mg^{2+}. Numerous studies have addressed the position and nature of binding sites for Na^+, Ca^{2+}, Zn^{2+}, and Mg^{2+} in the NMDAR ion permeation pathway (Burnashev et al., 1992; Mori et al., 1992; Premkumar and Auerbach, 1996; Sharma and Stevens, 1996a,b; Wollmuth et al., 1998; Antonov and Johnson, 1999; Fayyazuddin et al., 2000; see Zhu and Auerbach, 2001, in this issue). However, interactions between K^+ and the NMDAR channel have not been examined in detail, even though this ion is highly permeable and is normally present in the intracellular milieu at a high concentration. In this paper, we present information regarding the location and affinity of K^+ binding sites in recombinant NR1-NR2A NMDARs, inferred from the kinetics of Mg^{2+} block as a function of the extra- and intracellular concentrations of K^+.

Previous studies have demonstrated that Na^+ binds to two sites that are external to the Mg^{2+} binding site and that are accessible from both the intra- and extracellular solutions. Occupancy of these sites by Na^+ prevents the movement of extracellular Mg^{2+} between the extracellular compartment and the pore (i.e., blocks the association and "locks in" Mg^{2+}). We find that in addition to interacting with these external sites, K^+ binds to a site that is near the intracellular entrance of the permeation pathway. Occupancy of this internal site by K^+ reduces the rate constants for extracellular Mg^{2+} association and permeation, and increases the rate constant of Mg^{2+} dissociation back to the extracellular solution. Under physiological conditions, the interactions between K^+ and Mg^{2+} in the NMDA pore affect the affinity and voltage dependence of Mg^{2+} blockade.

Address correspondence to Anthony Auerbach, Department of Physiology and Biophysics, School of Medicine and Biomedical Sciences, SUNY at Buffalo, 124 Sherman Hall, Buffalo, NY 14214. Fax: (716) 829-2569; E-mail: auerbach@buffalo.edu.

[1]*Abbreviation used in this paper:* NMDAR, *N*-methyl-D-aspartate receptor.

MATERIALS AND METHODS

Wild-type rat cRNAs for the rat NR1 and NR2A subunits were expressed in *Xenopus* oocytes. Single-channel currents were recorded from outside-out patches. A detailed description of the molecular biology, expression protocols, electrophysiology, solutions, signal processing, kinetic analysis, and fitting procedures is given in Zhu and Auerbach (2001, in this issue).

RESULTS

The results are presented in four sections: first, the effects of intracellular K^+ ($[K^+]_{in}$) on Mg^{2+} dissociation and permeation; second, the effects of $[K^+]_{in}$ on Mg^{2+} association; third, the effects of extracellular K^+ ($[K^+]_{ex}$) on Mg^{2+} association; and fourth, the effects of $[K^+]_{ex}$ on Mg^{2+} dissociation and permeation.

Intracellular K^+ Increases the Mg^{2+} Dissociation Rate Constant and Decreases the Mg^{2+} Permeation Rate Constant

Increasing intracellular $[K^+]$ shortens the duration of the gaps arising from Mg^{2+} block (Fig. 1 A); i.e., Mg^{2+} is released from the NMDAR pore more rapidly when $[K^+]_{in}$ is elevated. The apparent Mg^{2+} release rate (k_{off})

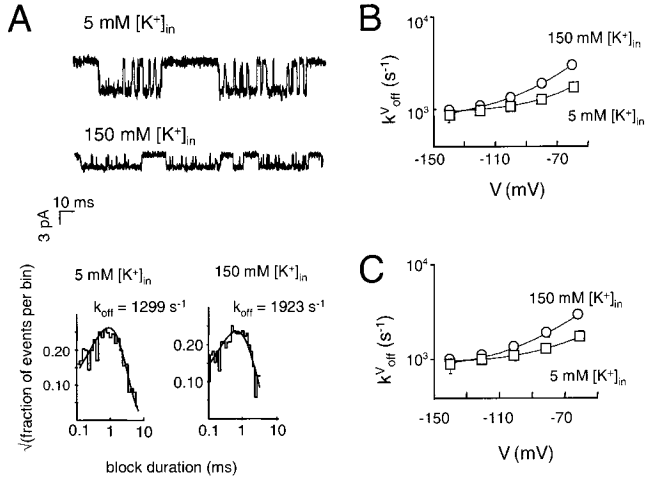

FIGURE 1. Effects of intracellular K^+ on Mg^{2+} release from the pore. (A) Single-channel currents showing Mg^{2+} block at different intracellular K^+ concentrations (50 mM Na^+ and 3 μM Mg^{2+} in the extracellular solution, V = −80 mV). The current amplitude is larger at lower $[K^+]_{in}$ because of a positive shift in the reversal potential. (Bottom) Closed interval duration histograms. The aggregate release rate of Mg^{2+} from the pore (k_{off}) increases with $[K^+]_{in}$. (B) Separating k_{off} into Mg^{2+} dissociation and permeation rate constants. The symbols are mean ± SD (usually, the SD was smaller than the symbol and is not visible) and were fitted using Eq. 1. The best-fit parameters are shown in Table I. (C) Model-based analysis of the effects of intracellular K^+ on Mg^{2+} dissociation and permeation. The two sets of data were simultaneously fitted by the sum of Eqs. 2 and 3. The solid lines are the predicted curves from the model with the best fit parameters (Table II).

is the sum of a dissociation rate constant back to the extracellular solution (k_{-Mg}) and a permeation rate constant (k_{pMg}). These two rate constants have opposite voltage dependencies: the former decreasing and the latter increasing with hyperpolarization. Fig. 1 B shows that between −60 and −120 mV, k_{off} increases with increasing $[K^+]_{in}$, as does its voltage dependence.

The effect of $[K^+]_{in}$ on Mg^{2+} dissociation and permeation was quantified by fitting k_{off} at different membrane potentials by:

$$k_{off}^{V} = k_{-Mg}^{0} e^{\frac{2\varepsilon V}{k_B T}} + k_{pMg}^{0}, \quad (1)$$

where V is the membrane potential, the superscript 0 indicates the salient rate constant at 0 mV, k_B is Boltzmann's constant, T is the absolute temperature (under our conditions, k_BT = 25.3 mV), and ε is the fractional electrical distance from the Mg^{2+} binding site to the top of the dissociation energy barrier. Results regarding Na^+ interactions with Mg^{2+} indicate that k_{pMg} is essentially voltage-independent (see Zhu and Auerbach, 2001, in this issue). Therefore, in Eq. 1, the fractional electrical distance from the Mg^{2+} binding site to the top of the permeation barrier was assumed to be zero.

TABLE I

The Effects of Intracellular [K^+] on the Apparent Rates of Mg^{2+} Dissociation and Permeation

$[K^+]_{in}$	k_{-Mg}^{0}	ε	k_{pMg}^{0}
mM	s^{-1}		s^{-1}
5	8,900 ± 2,400	0.49 ± 0.06	920 ± 32
150	19, 000 ± 1,700	0.44 ± 0.21	780 ± 38

$[K^+]_{in}$ is the intracellular K^+ concentration, k_{-Mg}^{0} is the Mg^{2+} dissociation rate constant with no membrane potential, ε is the electrical distance from the Mg^{2+} binding site to the peak of the dissociation barrier, and k_{pMg}^{0} is the Mg^{2+} permeation rate constant with no membrane potential (see Fig. 6 in companion article Zhu and Auerbach, 2001, in this issue). The results were obtained by fitting the experimental results of Fig. 1 B using Eq. 1. Mg^{2+} dissociates more rapidly, and permeates more slowly, in high $[K^+]_{in}$.

The result of fitting the experimental k_{off} values using Eq. 1 are shown in Table I. At 0 mV, k_{-Mg} is larger and k_{pMg} is smaller in 150 mM compared with 5 mM $[K^+]_{in}$; i.e., elevating intracellular $[K^+]$ enhances Mg^{2+} dissociation back to the extracellular space, but reduces Mg^{2+} permeation to the intracellular space.

The NMDAR channel has external binding sites that are able to bind Cs^+ and Na^+ (Antonov and Johnson, 1999). The effects of $[K^+]_{in}$ on the Mg^{2+} dissociation and permeation rate constants cannot, however, be explained by K^+ occupancy of these external sites because intracellular K^+ does not have access to the external sites when Mg^{2+} blocks the channel. Therefore, intracellular K^+ must be interacting with regions of the protein that are internal to the Mg^{2+} binding site. We assume the reduction in k_{pMg} with increasing $[K^+]_{in}$ occurs because the occupancy of this internal site by K^+ blocks the pathway for Mg^{2+} permeation into the intracellular compartment. Moreover, we speculate that the enhancement of k_{-Mg} with increasing $[K^+]_{in}$ may be caused by an electrostatic repulsion between the two ions.

To further quantify the effects of $[K^+]_{in}$ on Mg^{2+} dissociation, we used a model having one external Na^+ site and one internal K^+ site. The model assumes that Mg^{2+} cannot dissociate if the external site is occupied, and that Mg^{2+} dissociates at two different rate constants depending on whether or not the internal site is occupied. Accordingly, the apparent dissociation rate constant (k_{-Mg}^{V}) is described by:

$$k_{-Mg}^{V} = k_{-Mg1}^{0} e^{\frac{2\varepsilon V}{k_B T}} \left(1 + \frac{[K^+]_{in}}{J_{d,K_{in},internal}^{0} e^{\frac{-\beta V}{k_B T}}}\right)^{-1} \left(1 + \frac{[Na^+]_{ex}}{J_{d,Na_{ex}}}\right)^{-1} + k_{-Mg2}^{0} e^{\frac{2\varepsilon V}{k_B T}} \left(1 + \frac{J_{d,K_{in},internal}^{0} e^{\frac{-\beta V}{k_B T}}}{[K^+]_{in}}\right)^{-1} \left(1 + \frac{[Na^+]_{ex}}{J_{d,Na_{ex}}}\right)^{-1}. \quad (2)$$

$J_{d,Kin,internal}$ is the equilibrium dissociation constant of the internal site for intracellular K^+ (with Mg^{2+} in the

pore); k^0_{-Mg1} and k^0_{-Mg2} are the Mg^{2+} dissociation rate constants (at zero voltage and in the presence of extracellular $[Na^+]$) without and with a K^+ at the internal site, respectively; β is the fractional electrical distance from the intracellular solution to the internal K^+ binding site; and $J_{d,Na_{ex}}$ is the equilibrium dissociation constant of the lone external site for extracellular Na^+ when the pore is occupied by Mg^{2+}. The three experimental variables in Eq. 2 are $[K^+]_{in}$, $[Na^+]_{ex}$, and V.

Because extracellular Na^+ does not alter Mg^{2+} permeation (see Zhu and Auerbach, 2001, in this issue), this process can be described simply by:

$$k^V_{pMg} = \kappa^0_{pMg1}\left(1 + \frac{[K^+]_{in}}{J^0_{d,K_{in},internal}e^{\frac{-\beta V}{k_B T}}}\right)^{-1}, \quad (3)$$

where κ^0_{pMg1} is the intrinsic rate constant for Mg^{2+} permeation (with the internal site empty and no membrane potential), and k^V_{pMg} is the net Mg^{2+} permeation rate constant, which is a function of only two experimental variables, $[K^+]_{in}$ and V.

The experimental values of k^V_{off} were fitted by the sum of Eqs. 2 and 3, which has four free parameters (Table II). Fig. 1 C shows that the predicted curves match the experimental data, indicating that a single internal K^+ binding site is sufficient to explain the effects of $[K^+]_{in}$ on Mg^{2+} release from the pore. The Mg^{2+} dissociation rate constant is approximately seven times greater when there is a K^+ at the internal site compared with when this site is empty. The affinity of the internal site for K^+ when there is a Mg^{2+} in the pore is low, perhaps because of electrostatic repulsion between the ions. The internal K^+ binding site is ~84% through the electric field from the extracellular surface, and is ~24% deeper in the electric field than the Mg^{2+} binding site.

Intracellular K^+ Reduces the Mg^{2+} Association Rate Constant

In this section, we address the Mg^{2+} association rate constant as a function of intracellular $[K^+]$. Fig. 2 A shows that the open channel lifetimes are longer (i.e., the Mg^{2+} association rate constant is slower; Fig. 2 B) when $[K^+]_{in}$ is elevated. We first considered whether the apparent reduction in the Mg^{2+} association rate constant is caused exclusively by the binding of intracellular K^+ to the external monovalent cation sites. We made the simplifying assumptions that the two external sites are independent and identical, and that the occupancy of these sites by extracellular Na^+ is not voltage-dependent. Three sets of data, obtained at different $[K^+]_{in}$ (25, 50, and 100 mM) and at 100 mM $[Na^+]_{ex}$, were fitted simultaneously by:

$$k^V_{+Mg} = \kappa^0_{+Mg}e^{\frac{-2\delta V}{k_B T}}\left(1 + \frac{[Na^+]_{ex}}{K_{Na_{ex}}} + \frac{[K^+]_{in}}{K^0_{K_{in}}e^{\frac{-\alpha V}{k_B T}}}\right)^{-2}, \quad (4)$$

where κ^0_{+Mg} is the intrinsic Mg^{2+} association rate constant (i.e., in the absence of competing ions and with no membrane potential), $K_{Na_{ex}}$ and $K_{K_{in}}$ are the apparent dissociation constants for $[Na^+]_{ex}$ and $[K^+]_{in}$ at the external sites, respectively, (without Mg^{2+} in the pore), and α is the fractional electrical distance between the external binding sites and the intracellular compartment. Because Na^+ and K^+ can permeate, $K_{Na_{ex}}$ and $K_{K_{in}}$ are not true equilibrium constants. As can be seen in Fig. 2 C, the predicted curves provide a poor description of the experimental data. We conclude that in addition to the two external sites, there are other K^+ binding sites involved in the inhibition of the Mg^{2+} association rate constant.

As described above, intracellular K^+ increases the Mg^{2+} dissociation rate constant and decreases the Mg^{2+} permeation rate constant because it occupies an internal binding site that is close (in electrical distance) to the Mg^{2+} binding site. Therefore, we speculated that Mg^{2+} binds to the NMDAR pore only when both of the external sites and the internal site are empty. That is, we hypothesized that when K^+ occupies the internal site, the association rate constant for extracellular Mg^{2+} is significantly reduced.

TABLE II

Intracellular K^+ at the Internal Site: Equilibrium Dissociation Constant and Rate Constants for Mg^{2+} Dissociation and Permeation.

Parameter	Symbol	Units	Value
Equilibrium dissociation constant of the internal site for intracellular K^+ (Mg^{2+} present in the channel, no membrane potential)	$J^0_{d,K_{in},internal}$	mM	304 ± 60
Mg^{2+} dissociation rate constant (internal site empty, no membrane potential)	k^0_{-Mg1}	s^{-1}	8,343 ± 213
Mg^{2+} dissociation rate constant (internal site occupied, no membrane potential)	k^0_{-Mg2}	s^{-1}	62,513 ± 6,573
Electrical distance to the intracellular compartment	β		0.16 ± 0.07

The experimentally observed Mg^{2+} off rates measured at 150 mM and 5 mM $[K^+]_{in}$ and between −10 and −60 mV (Fig. 1 C) were simultaneously fitted by the sum of Eqs. 2 and 3. To restrict the number of free parameters, three terms were fixed at their previous estimates ($\kappa^0_{pMg} = 624\ s^{-1}$, $\varepsilon = 0.36$, and $J_{d,Na_{ex}} = 89$ mM). The estimate of k^0_{-Mg1} is similar to that obtained from experiments in different $[Na^+]$ (see Zhu and Auerbach, 2001, in this issue).

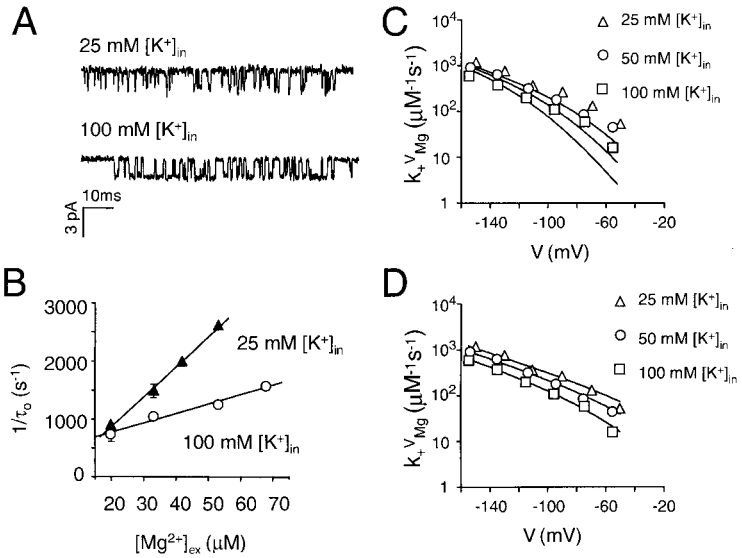

FIGURE 2. Effects of intracellular K^+ on the Mg^{2+} association rate constant. (A) Single-channel currents showing Mg^{2+} block at different intracellular K^+ concentrations. 100 mM Na^+ and 54 μM Mg^{2+} were present in the extracellular solution, and the membrane potential was −55 mV. Open times are longer in high $[K^+]_{in}$. (B) The inverse of open channel lifetime (τ_o) plotted as a function of the extracellular Mg^{2+} concentration. The decreased slope with the increased $[K^+]_{in}$ indicates that intracellular K^+ reduces the Mg^{2+} association rate constant. Where not shown, the SD is smaller than the symbol. (C) A global fit of experimental Mg^{2+} association rate constants using a model that allows intracellular K^+ to bind only to the two external monovalent cation sites (Eq. 4) does a poor job of describing the experimental results (Model Selection Criterion = 2.3). (D) A global fit of the same experimental data by a model that allows intracellular K^+ to bind to one internal site as well as the two external sites (Eq. 5) describes the experimental results (Model Selection Criterion = 4.3). The parameters for the best fit are shown in Table III.

To quantify the observations, we used a scheme that had four ion binding sites: two external sites that bind Na^+ or K^+; one intermediate site that is selective for Mg^{2+}; and one internal site that is selective for K^+. For simplicity, we assumed that occupancy of any one of the three monovalent cation binding sites completely prevents the association of extracellular Mg^{2+}. (Although the results given in Table II suggest that intracellular K^+ can bind to the internal site when the channel is blocked by Mg^{2+}, in the following analysis, we made the simplifying assumption that Mg^{2+} association is effectively eliminated when K^+ occupies the internal site.) A 12-state model is required to account for the effects of intracellular K^+ and extracellular Na^+ on the Mg^{2+} association rate constant, with six external site configurations (two Na^+, two K^+, one Na^+ and one K^+, one Na^+, one K^+, and empty) and two internal site configurations (one K^+ and empty).

We assume that the apparent association rate constant for Mg^{2+} is a function of the probability of all three of the monovalent cation sited being empty:

$$k^V_{+Mg} = \kappa^V_{+Mg}(P^e_{external})^2(P^e_{internal}),$$

where $P^e_{external}$ and $P^e_{internal}$ are the probabilities of the external sites and the internal site being empty. The apparent Mg^{2+} association rate constant is related to the experimental variables $[Na^+]_{ex}$, $[K^+]_{in}$, and V by:

$$k^V_{+Mg} = \kappa^0_{+Mg} e^{\frac{-2\delta V}{k_B T}} \left(1 + \frac{[Na^+]_{ex}}{K_{Na_{ex}}} + \frac{[K^+]_{in}}{K^0_{K_{in}} e^{\frac{-\alpha V}{k_B T}}}\right)^{-2} \left(1 + \frac{[K^+]_{in}}{K^0_{K_{internal}} e^{\frac{-\beta V}{k_B T}}}\right)^{-1}. \quad (5)$$

The first term in parentheses is the inhibition of Mg^{2+} association because of Na^+ and K^+ occupancy of the two external sites and the second term in parentheses is the inhibition because of K^+ occupancy of the single internal site. $K^0_{Kin,internal}$ is the apparent dissociation constant for intracellular K^+ at the internal site with no membrane potential. In the case of association, Mg^{2+} is not present in the pore yet and the monovalent ions are free to permeate. As stated before, the apparent affinities are not true dissociation equilibrium constants.

Fig. 2 D shows the results of fitting the experimental data using Eq. 5, with κ^0_{+Mg}, K^0_{Kin} and $K^0_{Kin,internal}$ as the only free parameters. The predicted curves match the experimental data. We conclude that a model having two external monovalent cation-binding sites and one internal K^+-selective site accounts for the effects of intracellular $[K^+]$ on Mg^{2+} association. The parameters for the best fit are shown in Table III.

Extracellular K^+ Decreases the Mg^{2+} Association Rate Constant

We next investigated the effects of extracellular K^+ on the Mg^{2+} association rate constant. Fig. 3 A illustrates single-channel currents recorded at two different extracellular K^+ concentrations ($[K^+]_{ex}$, 25 and 150 mM) in the presence of 100 mM intracellular Na^+. The channel open lifetime is longer at the higher $[K^+]_{ex}$, indicating that the Mg^{2+} association rate constant decreases with an increase in $[K^+]_{ex}$.

We again used the two-external, one-internal site model to quantify the results. We assumed that all three sites can bind extracellular K^+, and that occupancy of any one of these sites by K^+ effectively eliminates Mg^{2+} association. We also assumed that that Na^+ does not bind to the internal site.

TABLE III

Intracellular K^+ at the Monovalent Cation Sites: Apparent Dissociation Constants and the Rate Constant for Mg^{2+} Association

Parameter	Symbol	Units	Value
Dissociation constant of the external site for intracellular K^+ (Mg^{2+} not present in the channel, no membrane potential)	$K^0_{K_{in}}$	mM	8.3 ± 4.7
Dissociation constant of the internal site for intracellular K^+ (Mg^{2+} not present in the channel, no membrane potential)	$K^0_{K_{in},internal}$	mM	23 ± 4
Mg^{2+} association rate constant (external and internal sites empty, no membrane potential)	κ^0_{+Mg}	$M^{-1}s^{-1}$	$6.9 \times 10^8 \pm 0.3 \times 10^8$

The values were obtained by fitting Eq. 5 to the experimental Mg^{2+} association rates obtained at different $[K^+]_{in}$ and voltages (Fig. 2 D). The electrical distances ($\alpha = 0.83$, $\beta = 0.16$, and $\delta = 0.27$) and the apparent dissociation constant of the external site for extracellular Na^+ ($K_{Na_{ex}} = 42$ mM) were fixed at their previously determined values (see Zhu and Auerbach, 2001, in this issue). The estimate of the Mg^{2+} association rate constant in pure water is close to that obtained from experiments in different $[Na^+]_{ex}$ (see Zhu and Auerbach, 2001, in this issue).

For this model, we used an expression that relates the apparent association rate constant (k^V_{+Mg}) to $[K^+]_{ex}$, $[Na^+]_{in}$, and V:

$$k^V_{+Mg} = \kappa^0_{+Mg} e^{\frac{-2\delta V}{k_B T}} \left(1 + \frac{[K^+]_{ex}}{K_{K_{ex}}} + \frac{[Na^+]_{in}}{K^0_{Na_{in}} e^{\frac{-\alpha V}{k_B T}}}\right)^{-2} \left(1 + \frac{[K^+]_{ex}}{K^0_{K_{ex}internal} e^{\frac{(1-\beta)V}{k_B T}}}\right)^{-1}. \quad (6)$$

Fig. 3 D shows experimental k^V_{+Mg} values obtained at three different $[K^+]_{ex}$ as a function of the membrane potential, fitted simultaneously by Eq. 6. The fitting results are given in Table IV. The fitted curves provide a good description of the experimental data, indicating that a model with two external sites that can bind either Na^+ or K^+, and with one internal site that is K^+-selective, accounts for the effects of extracellular Na^+ and K^+ on the Mg^{2+} association rate constant.

In the absence of a membrane potential, the internal site has an extremely low apparent affinity for extracellular K^+. To evaluate the significance of extracellular K^+ occupancy of the internal site with regard to Mg^{2+} association, we fitted the same experimental data using a model that allowed K^+ to bind only to the external sites. The equations for this fit were the same as were used to describe the effects of extracellular Na^+ on Mg^{2+} association (see Zhu and Auerbach, 2001, in this issue). The results show that the fit using this scheme (Fig. 3 C; Model Selection Criterion = 4.6) is significantly worse than the fit by Eq. 6 (Fig. 3 D; Model Selection Criterion = 5.4). Without the incorporation of an

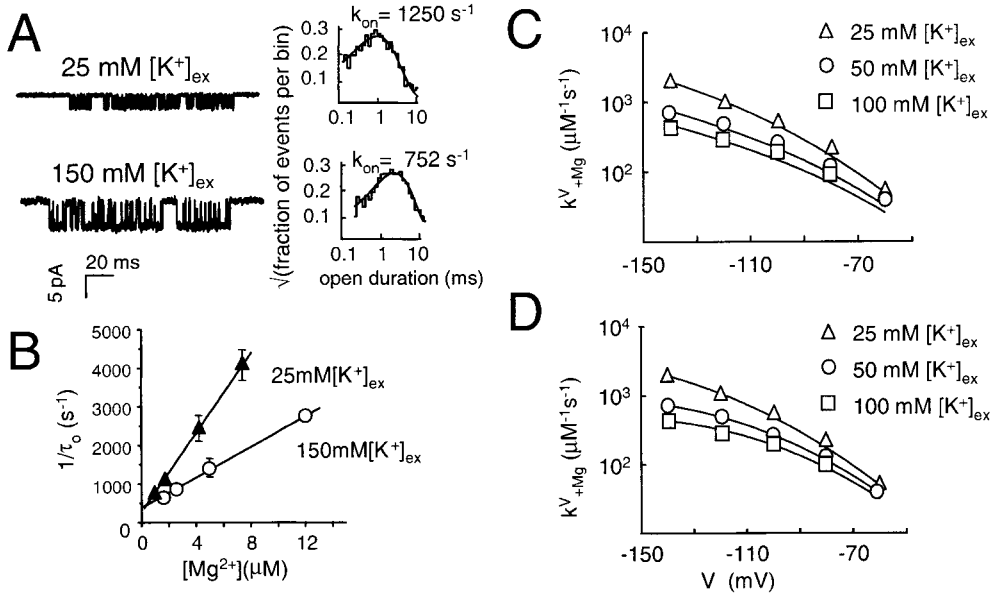

FIGURE 3. Effects of extracellular K^+ on the Mg^{2+} association rate constant. (A) Single-channel currents at different extracellular K^+ concentrations (2 μM Mg^{2+} in the extracellular solution; the intracellular solution contained 150 mM Na^+; V = −100 mV). (B) The inverse of open channel lifetime plotted as a function of Mg^{2+} concentration. The decreased slope with increasing $[K^+]_{in}$ indicates that extracellular K^+ reduces the Mg^{2+} association rate constant. (C) Fits of the experimental Mg^{2+} association rate constants using a model where extracellular K^+ binds only to the two external sites. (see Eq. 3 from Zhu and Auerbach, 2001, in this issue; Model Selection Criterion = 4.6). (D) Fits of the experimental Mg^{2+} association rate constants using a model where extracellular K^+ binds to two external sites and one internal site (Eq. 6; Model Selection Criterion = 5.4). Parameters for the best fit are shown in Table IV. The model with two external and one internal binding site for extracellular K^+ is superior. The SDs are all smaller than the symbol.

TABLE IV

Extracellular K^+ at the Monovalent Cation Sites: Apparent Dissociation Constants and the Rate Constant for Mg^{2+} Association

Parameter	Symbol	Units	Value
Dissociation constant of the external site for extracellular K^+ (Mg^{2+} not present in the channel)	$K_{K_{ex}}$	mM	151 ± 25
Dissociation constant of the internal site for extracellular K^+ (Mg^{2+} not present in the channel, no membrane potential)	$K^0_{K_{ex,internal}}$	M	16 ± 0.5
Mg^{2+} association rate constant (external and internal sites empty, no membrane potential)	κ^0_{+Mg}	$M^{-1}s^{-1}$	$2.0 \times 10^8 \pm 0.1 \times 10^8$

The values were obtained by fitting Eq. 6 to the experimental Mg^{2+} association rates obtained at different intracellular $[K^+]$ and voltages (Fig. 3 C). To restrict the number of free parameters, the three electrical distances ($\delta = 0.27$, $\alpha = 0.83$, and $\beta = 0.16$) and the dissociation constant of the external site for intracellular Na^+ ($K^0_{d\,Na_{in}} = 5$ mM) were fixed at their previous estimates (see Zhu and Auerbach, 2001, in this issue). At −120 mV, $K^0_{K_{ex,internal}} = 300$ mM.

internal K^+ binding site, the predicted curves deviate from the experimental results because of an overestimation of the voltage dependence of k^V_{+Mg}. The small apparent voltage dependence of k^V_{+Mg} can be attributed to voltage-dependent binding of extracellular K^+ to the internal sites, which are deep within the electric field. Hyperpolarization increases Mg^{2+} association, but also enhances the occupancy of the internal site by extracellular K^+, which in turn serves to reduce the Mg^{2+} association rate constant. Thus, the results support the conclusion that extracellular K^+ binds to both the external sites and the internal site.

Extracellular K^+ Reduces the Mg^{2+} Dissociation Rate Constant but Increases the Mg^{2+} Permeation Rate Constant

Extracellular K^+ and Na^+ have different effects on the kinetics of Mg^{2+} unbinding. $[Na^+]_{ex}$ reduces the rate of Mg^{2+} release from the channel. In contrast, $[K^+]_{ex}$ shortens the gaps in the single-channel record that reflect sojourns of Mg^{2+} in the channel (Fig. 4 A), indicating that extracellular K^+ increases the rate of Mg^{2+} release. In addition, the blocking gaps are longer-lived in equivalent concentrations of Na^+ versus K^+, which further highlights the distinct effects of these two cations.

Fig. 4 B shows k_{off} measured at different $[K^+]_{ex}$ over a wide range of membrane potentials. (In these experiments, there was no extracellular $[Na^+]$). k_{off} increases with increasing $[K^+]_{ex}$ between −100 and −140 mV. However, the difference between k_{off} in 25 vs. 150 mM $[K^+]_{ex}$ becomes smaller as the membrane is depolarized, until it disappears entirely at about −80 mV.

We assume that extracellular K^+ binding to the external sites is voltage-independent. The apparent Mg^{2+} dissociation and permeation rate constants were ob-

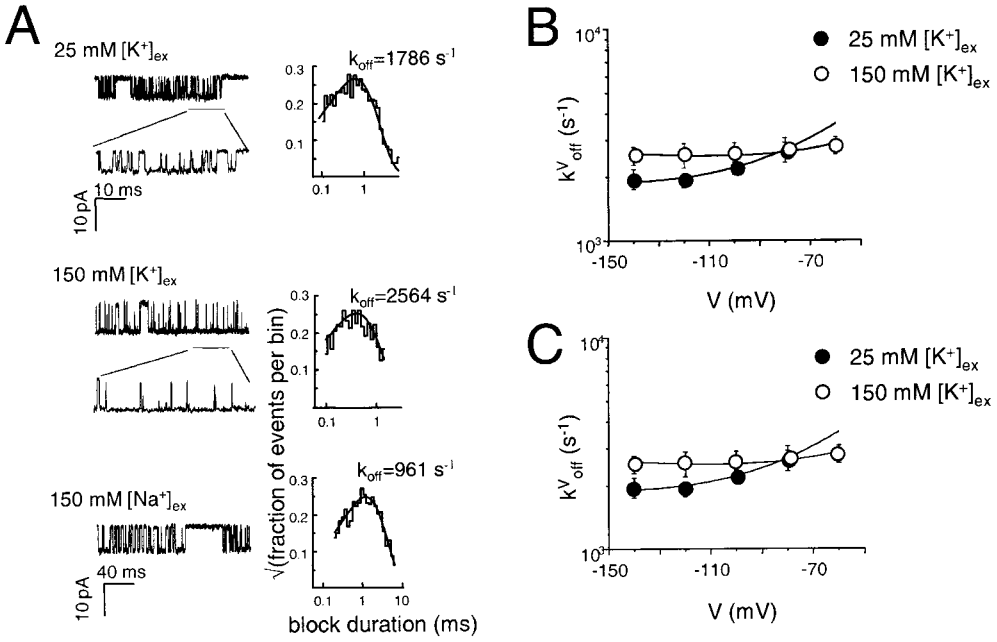

FIGURE 4. Effects of extracellular K^+ on the Mg^{2+} off rate constant. (A) Single-channel currents showing Mg^{2+} block at different extracellular K^+ concentrations (3 μM extracellular Mg^{2+}, 100 mM intracellular Na^+; V = −140 mV). Closed interval duration histograms are shown to the right. k_{off} increases with increasing $[K^+]_{ex}$, and is larger in equivalent concentrations of extracellular K^+ compared with Na^+. (B) Separating k_{off} into the Mg^{2+} dissociation and permeation rate constants. Solid lines are fits by Eq. 1. The best-fit parameters are shown in Table V. (C) Model-based analyses of the Mg^{2+} dissociation and permeation rate constants as a function of $[K^+]_{ex}$. The k_{off} values from both K^+ concentrations were simultaneously fitted by the sum of Eqs. 7 and 9. The best-fit parameters are shown in Table III ($n = 2$).

TABLE V

The Effects of Extracellular [K⁺] on the Apparent Rate Constants for Mg^{2+} Dissociation and Permeation

$[K^+]_{ex}$	k^0_{-Mg}	ε	k^0_{pMg}	λ
mM	s^{-1}		s^{-1}	
25	$1.2 \times 10^4 \pm 10^3$	0.36	$1.2 \times 10^3 \pm 44$	0.03
150	$4.5 \times 10^3 \pm 4.7 \times 10^2$	—	$1.8 \times 10^3 \pm 35$	—

$[K^+]_{ex}$ is the extracellular K^+ concentration, and λ is the electrical distance from the Mg^{2+} binding site to the peak of the barrier for Mg^{2+} permeation (other parameters defined in Table I). The results were obtained by fitting the experimental results in Fig. 1 B by Eq. 1.

tained by fitting with Eq. 1. The results are shown as solid lines in Fig. 4 B, using the parameters in Table V. k^0_{-Mg} is substantially lower in high $[K^+]_{ex}$ (a "lock-in" effect), whereas k^0_{pMg} is slightly higher in high $[K^+]_{ex}$ (a "kick-out" effect).

We again analyzed the results using schemes in which extracellular K^+ can bind to two external sites and one internal site. Accordingly, only the external sites are involved in the modulation of Mg^{2+} unbinding because the presence of a bound Mg^{2+} prevents the access of extracellular ions to the internal site. With Na^+, the data could be described assuming that only one external site was available when Mg^{2+} was present in the pore. For the K^+ experiments, we used models (having either one or two external sites) that assumed that Mg^{2+} dissociates back to the extracellular solution only when all of the external sites are vacant:

$$k^V_{-Mg} = k^0_{-Mg} e^{\frac{2\varepsilon V}{k_B T}} \left(1 + \frac{[K^+]_{ex}}{J_{K_{ex}}}\right)^{-n}. \quad (7)$$

The quantitative analysis of the effects of $[K^+]_{ex}$ on Mg^{2+} permeation is more complex because this process could be differentially affected in the case of zero, one, or two K^+ bound to the external sites. We use three different models to fit the data.

First, we assumed that only one extracellular K^+ binds when the pore is blocked by Mg^{2+}. Thus, the observed Mg^{2+} permeation rate constant (k^V_{pMg}) is the weighted average of only two components, the permeation rate constant without ($k^V_{0,pMg}$) and with ($k^V_{1,pMg}$) a bound K^+:

$$k^V_{pMg} = k^0_{0,pMg} e^{\frac{-2\lambda V}{k_B T}} \left(1 + \frac{[K^+]_{ex}}{K_{K_{ex}}}\right)^{-1} + k^0_{1,pMg} e^{\frac{-2\lambda V}{k_B T}} \left(\frac{K_{K_{ex}}}{[K^+]_{ex}}\right)^{-1}. \quad (8)$$

Note that we have assumed that the voltage dependence of Mg^{2+} permeation (given by the electrical distance parameter, λ) is the same regardless of the occupancy status of the external site. The observed net Mg^{2+} release rate (k^V_{off}) as a function of $[K^+]_{ex}$, and V was fitted by the sum of Eq. 7 (with $n = 1$) and Eq. 8. The best-fit parameters (Table VI) indicate that, with this scheme, the Mg^{2+} permeation rate constant is approximately three times greater when there is a K^+ at the external site compared with that when this site is empty.

The second model assumed that extracellular K^+ occupies either of two external sites, but that the occupancy of only one influences Mg^{2+} permeation:

$$k^V_{pMg} = k^0_{0,pMg} e^{\frac{-2\lambda V}{k_B T}} \left(1 + \frac{[K^+]_{ex}}{J_{K_{ex}}}\right)^{-2} + k^0_{1,pMg} e^{\frac{-2\lambda V}{k_B T}} \left[2\left(1 + \frac{J_{K_{ex}}}{[K]^+_{ex}}\right)^{-1}\left(1 + \frac{[K]^+_{ex}}{J_{K_{ex}}}\right)^{-1} + \left(\frac{[K]^+_{ex}}{J_{K_{ex}\,ex}}\right)^{-2}\right]. \quad (9)$$

The observed Mg^{2+} release rate (k^V_{off}) as a function of $[K^+]_{ex}$, and V was again fitted simultaneously by the sum of Eqs. 7 (with $n = 2$) and 9. The best-fit parameters (Table VI) indicate that, with this scheme, the Mg^{2+} permeation rate constant again is more than two times greater when there is a K^+ at the external site compared with that when this site is empty.

TABLE VI

Extracellular K^+ at the External Cation Site: The Equilibrium Dissociation Constant and the Rate Constants for Mg^{2+} Dissociation and Permeation

Parameter	Symbol	Units	Value	
No. of external K^+ sites	n		1 (fixed)	2 (fixed)
Equilibrium dissociation constant site for extracellular K^+ at the external site (Mg^{2+} present in the channel)	$J_{d,K_{ex}}$	mM	48.2 ± 15.0	168.7 ± 32.0
Mg^{2+} dissociation constant with external site(s) empty (no membrane potential)	k^0_{-Mg}	s^{-1}	18,700 ± 3,100	16,197 ± 1,827
Mg^{2+} permeation rate constant (no membrane potential)	$\kappa^0_{0,pMg}$	s^{-1}	723 ± 182	908 ± 97
	$\kappa^0_{1,pMg}$	s^{-1}	2,130 ± 47	2,130 ± 47
Goodness of fit	MSC		2.81	2.81

The results of the obtained by fitting to the results shown in Fig. 4 using the sum of Eq. 7 ($n = 1$) and Eq. 8, or Eq. 7 ($n = 2$) and Eq. 9. The electrical distances and the dissociation constant of the external site(s) for extracellular Na^+ and K^+ were fixed at their previously determined values. The Mg^{2+} permeation rate constant increases when K^+ is present in the external portion of the permeation pathway.

Finally, we attempted to use a model where the occupancy of two external sites influences both dissociation and permeation, so that the observed Mg^{2+} permeation rate constant is a weighted average of three components:

$$k^0_{pMg} = k^0_{0,pMg} e^{\frac{-z\lambda V}{k_B T}} \left(1 + \frac{[K^+]_{ex}}{K_{d,K_{ex}}}\right)^{-2} + k^0_{1,pMg} e^{\frac{-z\lambda V}{k_B T}} 2\left(1 + \frac{[K^+]_{ex}}{K_{d,K_{ex}}}\right)^{-1}\left(1 + \frac{K_{d,K_{ex}}}{[K^+]_{ex}}\right)^{-1} + k^0_{2,pMg} e^{\frac{-z\lambda V}{k_B T}} \left(1 + \frac{K_{d,K_{ex}}}{[K^+]_{ex}}\right)^{-2}. \quad (10)$$

The fit by the sum of Eq. 7 (with $n = 2$) and Eq. 10 to the observed Mg^{2+} "off" rates would not converge. There was a large SD in the estimated value of $k^0_{2,pMg}$ even after constraining $k^0_{0,pMg}$.

In summary, the occupancy of the external site(s) by K^+ increases the Mg^{2+} permeation rate constant by about a factor of three. The analysis does not allow us to distinguish if there are one or two such sites, and, in the case of two sites, if double occupancy alters Mg^{2+} permeation to a different extent than single occupancy.

A Qualitative Assessment of the Affinity and Selectivity of the Internal Site

In contrast to the external sites, we hypothesize that the internal site specifically binds K^+. The low relative affinity of the internal site for intracellular Na^+ versus K^+ is immediately apparent in Fig. 5, which shows the voltage dependence of k_{+Mg}. At −140 mV, k_{+Mg} is the same in 100 and 5 mM $[Na^+]_{in}$ (Fig. 5 A). This is because there is very little binding of intracellular Na^+ to either the external or internal sites at this hyperpolarized potential. (The external site has an apparent dissociation constant of 532 mM for intracellular Na^+ at −140 mV; see Zhu and Auerbach, 2001, in this issue) However, at –80 mV, k_{+Mg} is 1.6 times smaller in 100 mM vs. 5 mM $[Na^+]_{in}$. This is because, upon depolarization, intracellular Na^+ increasingly occupies the external sites (after crossing the entire electric field) and increasingly inhibits Mg^{2+} association. The significantly higher voltage dependence in high intracellular Na^+ is evidence that intracellular Na^+ binds mainly to the external sites, and that the affinity of the internal site for Na^+ is so low that it can be ignored.

In contrast, the internal site has a relatively high affinity for K^+. Fig. 5 B shows that $[K^+]_{in}$ inhibits Mg^{2+} association at hyperpolarized potentials, and that this inhibition does not show a strong voltage dependence. This is a reflection of the weak voltage dependence of the occupancy of the internal site by intracellular K^+. (The internal site apparent affinity for intracellular K^+ increases only from 23 mM at 0 mV to 55 mM at −140 mV). We conclude that intracellular Na^+ binds mainly to the external sites, whereas intracellular K^+ binds to a significant extent to both the internal and the external sites.

Fig. 5 also illustrates that the internal site also selects for K^+ over Na^+ when these ions originate from the extracellular compartment. The inhibition of k_{+Mg} by extracellular Na^+ shows only a slight voltage dependence (Fig. 5 C), whereas the inhibition by extracellular K^+ shows a strong voltage dependence (Fig. 5 D). This is consistent with the interpretation that extracellular Na^+ binds mainly to the external sites, whereas extracellular K^+ binds both to the external sites as well as to the internal site, which lies deep in the electric field.

DISCUSSION

Ion Binding Sites in the NMDAR Permeation Pathway

Fig. 6 shows a fanciful representation of the ion binding sites in the NMDAR pore, motivated by the close

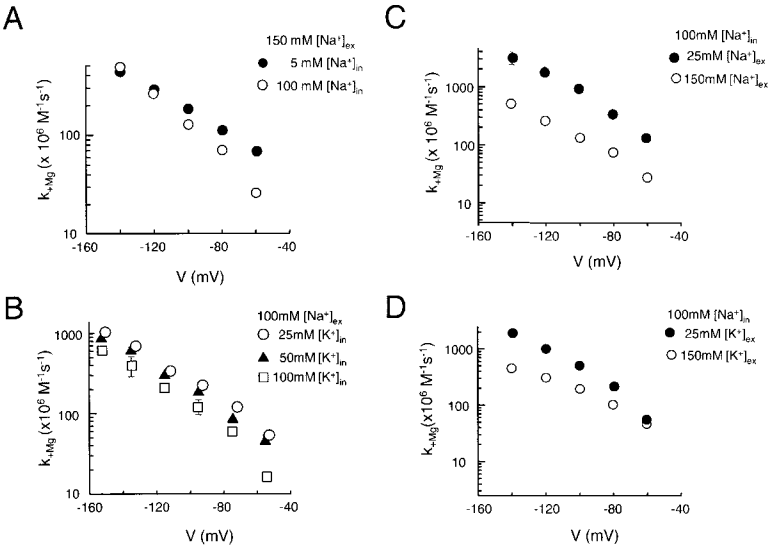

FIGURE 5. The distinct effects of Na^+ and K^+ on the voltage dependence of Mg^{2+} association reflect the locations of the monovalent cation-binding sites. (A) The inhibition of k_{+Mg} by $[Na^+]_{in}$ is voltage-dependent because intracellular Na^+ must cross the entire electric field to occupy the external sites. (B) The inhibition of k_{+Mg} by $[K^+]_{in}$ is only weakly voltage-dependent between −140 and −80 mV because, in this range, intracellular K^+ blocks Mg^{2+} association via the occupancy of the internal site. The large inhibition at −55 mV arises from K^+ occupancy of the external site. (C) The inhibition of k_{+Mg} by $[Na^+]_{ex}$ is not voltage-dependent because extracellular Na^+ does not have to enter the entire electric field to occupy the external sites. (D) The inhibition of k_{+Mg} by $[K^+]_{ex}$ is voltage-dependent because extracellular K^+ can cross the entire electric field to occupy the internal site. Its occupancy of the external sites is significant, but voltage-independent.

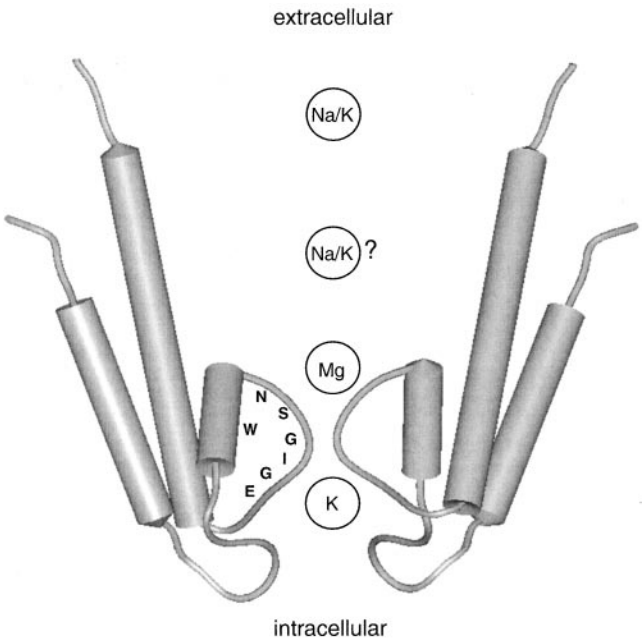

FIGURE 6. A representation of the ion binding sites in the NMDA receptor channel. The protein is a modified structure of KcsA (Doyle, et al., 1998), drawn upside down (Wood et al., 1995) and with a wide extracellular entrance. The large intra- and extracellular domain of the NMDAR are not shown. The amino acid sequence is that of the NR1 subunit; the homologous region (N to C) is TVGYGD in KcsA and GluR0, and NSPVPQ in NR2A. The four regions where Na^+, K^+, and Mg^{2+} linger during their passage through the channel are drawn as circles. There are two monovalent cation-binding sites in the external portion of the permeation pathway. The location of one of these external sites (indicated by a question mark) is undetermined, and could be either beyond the extracellular margin or deep within of the electric field. Under physiological conditions, these sites are occupied both by Na^+ (mainly from the extracellular solution) and K^+ (mainly from the intracellular solution). There is a Mg^{2+} binding site located 0.60 through the electric field from the extracellular solution. The equilibrium dissociation constant of this site for Mg^{2+} (in the absence of competing ions and with no membrane potential) is 12 μM. Extracellular Mg^{2+} associates rapidly to this site ($\sim 5 \times 10^8$ $M^{-1}s^{-1}$), thus, motivating the wide extracellular entrance. There is an internal, K^+-selective site located 0.16 through the electric field from the intracellular solution. Access to the Mg^{2+} site from the extracellular solution is reduced by monovalent cation occupancy of either the internal site or the external sites. Occupancy of one external site (by Na^+ or K^+) prevents Mg^{2+} dissociation, and occupancy of the internal site (by K^+) prevents Mg^{2+} permeation and increases the rate constant of Mg^{2+} dissociation back to the extracellular solution. The apparent voltage dependence of Mg^{2+} blockade strongly depends on the occupancies of the three monovalent cation-binding sites. Under standard conditions (140 mM $[Na^+]_{ex}$, 5 mM $[Na^+]_{in}$, 2 mM $[K^+]_{ex}$, and 140 mM $[K^+]_{in}$; V = −60 mV, 23°C, no extracellular Mg^{2+}), the external sites are occupied by at least one monovalent cation with $P = 0.978$, and the internal site is occupied by K^+ with $P = 0.806$.

structural (Wood et al., 1995) and evolutionary (Chen et al., 1999) relationship between K^+ channels (which are shaped like an inverted teepee; Doyle et al., 1998) and cation-selective glutamate receptor channels. When the channel is free of Mg^{2+}, Na^+, and K^+ interact with two sites that are located in the external portion of the permeation pathway. Either both monovalent cation sites are located outside the electric field, or one is outside and the other is about midway through the electric field (see Zhu and Auerbach, 2001, in this issue), perhaps in a central cavity. K^+ also lingers at an additional site that is in the internal portion of the permeation pathway. As a fraction of the electric field (from the extracellular solution), the Mg^{2+} site is at ∼0.60, and the internal, K^+-selective site is at ∼0.84.

Although we can estimate the locations of the ion-binding sites in terms of their electrical distance, we can only guess at their physical locations in the protein. The amino acid sequences in the vicinity of the selectivity filter for representative glutamate receptor and K^+ channel subunits are as follows:

```
KcsA    TTVGYGDL
G1uR0   TTVGYGDR
NR1      LNSGIGEG
NR2A     NNSVPVQN
```

In KcsA, Ba^{2+} binds to the channel at the juncture of the selectivity filter and the central cavity (Jiang and MacKinnon, 2000) near a threonine (Doyle et al., 1998). In the NMDAR NR1 subunit, the homologous residue in the sequence is an asparagine, the mutation of which has only a modest effect on Mg^{2+} block but substantially alters Ca^{2+} permeability (Burnashev et al., 1992; Wollmuth et al., 1998). The sequence of the NR2A subunit is not conserved, but mutation of the second of the vicinal asparagines has a strong inhibitory effect on Mg^{2+} binding (Mori et al., 1992; Sharma and Stevens, 1996a; Wollmuth et al., 1998). In terms of electrical distances, the Ba^{2+} site of potassium channels is ∼30% from the internal solution, whereas the Mg^{2+} site of the NMDAR is ∼60% from the external solution.

The location of the superficial external monovalent cation site is more difficult to pinpoint. It may be formed by the NH_2-terminal domain up to M1 and the M3-M4 linker (Beck et al., 1999), and may perhaps relate to external Zn^{2+}-binding residues (Fayyazuddin et al., 2000). The lack of voltage dependence in the occupancy of this site is different from that of the internal lock-in site of K^+ channels, which are ∼30% through the field from the intracellular solution (Neyton and Miller, 1988).

The internal K^+ site of NMDAR appears to be homologous to the external lock-in site of potassium channels, as both are ∼15% through the field from the closest bulk solution. In NMDAR, this site may be located in the filter or in an inner vestibule formed by M2 residues (Kuner et al., 1996). Mutation of the second glycine in the NR1 sequence, and the final asparagine in

the NR2A sequence, reduces the channel conductance for outward current carried by Cs^+ (Kupper et al., 1996), thus these residues are candidates for the internal site. Mutation of the glutamate in NR1 and the glutamine in NR2A (to lysine) also decreases block by internal Mg^{2+}, but these residues are less attractive candidates because they are not accessible to intracellular sulfhydryl reagents (Kuner et al., 1996). A tryptophan residue in both NR1 and NR2 subunits modulates Mg^{2+} block (Williams et al., 1998) and may also influence the internal K^+ site. In NMDAR, as in K^+ channels, this lock-in site is more selective than the corresponding one on the other face of the permeation pathway.

Although the results and analyses clearly indicate that there are at least three K^+ binding sites in the NMDAR channel (two external and one internal), there are certain inconsistencies in the parameter values that suggest that the situation is more complex. First, there is a substantial spread in the estimated rate constant for Mg^{2+} association in the absence of a membrane potential and competing ions. The value obtained from varying $[K^+]_{ex}$ was $2.0 \pm 0.1 \times 10^8$ $M^{-1}s^{-1}$ (Table IV), whereas that obtained from varying $[Na^+]_{ex}$ was $7.8 \pm 2.4 \times 10^8$ $M^{-1}s^{-1}$ (see Table I in Zhu and Auerbach, 2001, in this issue). Second, for both Na^+ and K^+, the apparent affinities of the external sites are higher for intra- versus extracellular ions. However, the parameters indicate that intracellular Na^+ associates 8 times faster, whereas K^+ associates 18 times faster than its extracellular counterpart, even though these two ions have similar reversal potentials and conductances (Zhu, Y., and A. Auerbach, unpublished observations). Third, the results show that whereas intracellular K^+ has ready access to the external sites (K^0_{Kin} = 8.3 mM; Table III), extracellular K^+ has an extremely low affinity for the internal site ($K^0_{Kex,internal}$ = 16 M; Table IV). We cannot give specific reasons for these inconsistencies. It is possible that Na^+ and K^+ can differentially alter the shape and/or properties of the permeation pathway via a direct interaction with the protein, as has been proposed for K^+ channels (Immke et al., 1999). In addition, it is likely that at least some of the basic assumptions of the analysis, e.g., discrete barriers, ion independence and single-filing, are not accurate in detail.

Comparison with Previous Results

Our results agree with those of Antonov et al. (1998) and Antonov and Johnson (1999) with regard to the number and the relative locations in the electric field of the NMDAR external monovalent ion-binding sites, and the effect of occupancy of these sites on the kinetics of Mg^{2+} blockade. One difference is that we observe that occupancy of an internal site by intracellular K^+ accelerates Mg^{2+} dissociation limits Mg^{2+} permeation, whereas Antonov and Johnson (1999) did not observe any effect of intracellular Cs^+ on the Mg^{2+} net unbinding rate constant. This difference can perhaps be traced to the difficulty in detecting the effect of intracellular monovalent ions on the kinetics of Mg^{2+} blockade. First, the increased rate of Mg^{2+} dissociation and decreased rate of Mg^{2+} permeation offset, to some extent. That is, the effect of intracellular permeant ions on the net Mg^{2+} release rate is small. Second, electrostatic repulsion between the bound Mg^{2+} and the ion at the internal site decreases the affinity of internal site. As a consequence, this site has a very low affinity for intracellular ions. Third, extracellular Na^+ reduces Mg^{2+} dissociation by binding to the external site. Thus, in the presence of a high concentration of extracellular Na^+, the enhancement of Mg^{2+} dissociation by the intracellular permeant ion is obscured. In our experiments, $[Na^+]_{ex}$ was low (50 mM), specifically to minimize this effect. Antonov and Johnson (1999) used a high $[Na^+]_{ex}$ (140 mM), which is perhaps the main reason why a change in the Mg^{2+} unbinding rate in different $[Cs^+]_{in}$ was not observed. Finally, given the high selectivity of the internal site for K^+ over Na^+, it is possible that this site has a low affinity for Cs^+.

The Effect of Physiological Concentrations of Intracellular K^+ on the Apparent Parameters of Mg^{2+} Block

In contrast to the voltage-independent binding of extracellular Na^+ to the external sites, the binding of intracellular K^+ to both the external sites and the internal site is voltage-dependent. Therefore, under physiological conditions, intracellular K^+ will have a significant influence on the apparent voltage dependence of Mg^{2+} block.

In the presence of 140 mM K^+ in the intracellular solution (and without any permeant ions in the extracellular solution), k^V_{+Mg} can be described by Eq. 5 (with $[Na^+]_{ex} = 0$). Using the values in Table I, we used this equation to compute apparent association rate constants in 140 mM intracellular K^+ ($k^V_{+Mg,\,140}$) between −60 to −140 mV). These were fitted by a standard exponential function to estimate the apparent voltage dependence (δ_{140}):

$$k^V_{+Mg,140} = k^0_{+Mg,140} e^{\frac{-\zeta_{140} V}{k_B T}}. \qquad (11)$$

The fitted parameters were $k^0_{+Mg,140} = 1.4 \times 10^6$ $M^{-1}s^{-1}$ and $\delta_{140} = 0.75$. This voltage dependence is about threefold greater than the intrinsic voltage dependence of Mg^{2+} association ($\delta = 0.24$; see Zhu and Auerbach, 2001, in this issue). In 140 mM $[K^+]_{in}$, the Mg^{2+} association rate constant is only ~0.2% of its value in pure water at 0 mV, but it is 2% of this value at −60 mV. Physiological concentrations of intracellular K^+ increase the apparent voltage dependence of Mg^{2+} association primarily as a consequence of voltage-dependent occupancy of the external site.

A similar approach was used to examine the effect of intracellular K^+ on Mg^{2+} dissociation and permeation. The apparent Mg^{2+} dissociation rate is given by Eq. 2 (with $[Na^+]_{ex} = 0$). Using the values in Table I and this equation to compute $k^V_{-Mg,140}$ values, and then fitting these by an exponential function (see Eq. 11), we estimate $k^0_{-Mg,140} = 2.4 \times 10^4\ s^{-1}$ and $\xi_{140} = 0.40$. Thus, 140 mM $[K^+]_{in}$ alone increases the magnitude of the apparent Mg^{2+} dissociation rate constant approximately threefold (at 0 mV), but does not influence the apparent voltage dependence of this process ($\varepsilon = 0.35$; see Zhu and Auerbach, 2001, in this issue).

The effect of extracellular Na^+ on Mg^{2+} permeation is small (see Zhu and Auerbach, 2001, in this issue). However, occupancy of the internal site by K^+ prevents Mg^{2+} permeation, thus, the effect of intracellular K^+ on Mg^{2+} permeation is expected to be significant. The apparent Mg^{2+} permeation rate constant is given by Eq. 3 (with $[Na^+]_{ex} = 0$). Proceeding as above, we estimate $k^0_{pMg,140} = 427\ s^{-1}$ and $\xi_{140} = 0.05$. Thus, 140 mM $[K^+]_{in}$ alone decreases the magnitude of the Mg^{2+} permeation rate by ~30% of its value in pure water (at 0 mV), but has only a small effect on the apparent voltage dependence of this process $\lambda = 0.35$; see Zhu and Auerbach, 2001, in this issue).

We combined the apparent values of the Mg^{2+} block to estimate an apparent Mg^{2+} equilibrium dissociation constant. The results were $K^0_{d\,Mg,140} = 17$ mM and $\xi_{140} = 1.13$, compared with the intrinsic values of 12 μM and 0.57, respectively (see Zhu and Auerbach, 2001, in this issue). Thus, 140 mM $[K^+]_{in}$ alone causes a >1,400-fold increase in the apparent Mg^{2+} equilibrium dissociation constant (at 0 mV), and approximately doubles the voltage dependence of equilibrium blockade.

The results suggest that the three monovalent cation-binding sites in the NMDAR permeation pathway serve two basic functions. First, they contribute to the selectivity and the conductance of the channel to Na^+ and K^+ in ways that remain to be quantified. We hope that our results will serve as a guide for future studies of permeant ion movement through the NMDAR pore. Second, the equilibrium occupancies of the external and internal sites have a strong influence on the magnitude and voltage dependence of Mg^{2+} block. It is possible that fluctuations in the concentrations of Na^+ and K^+ in the synaptic gap and/or dendrite regulate the kinetics and equilibrium blockade of NMDAR at synapses.

We thank Thomas Kuner and Peter Seeburg for the rat NR1 and NR2A subunit cDNAs, and Jon Johnson for insightful comments on the manuscript.

This work was supported by a grant to A. Auerbach (NS-86554.)

Submitted: 26 May 2000
Revised: 24 January 2001
Accepted: 25 January 2001

REFERENCES

Antonov, S.M., V.E. Gimiro, and J.W. Johnson. 1998. Binding sites for permeant ions in the channel of NMDA receptors and their effects on channel block. *Nat. Neurosci.* 1:451–461.

Antonov, S.M., and J.W. Johnson. 1999. Permeation ion regulation of *N*-methyl-D-aspartate receptor channel block by Mg^{2+}. *Proc. Natl. Acad. Sci. USA.* 96:14571–14576.

Beck, C., L.P. Wollmuth, P.H. Seeburg, B. Sakmann, and T. Kuner. 1999. NMDAR channel segments forming the extracellular vestibule inferred from the accessibility of substituted cysteines. *Neuron.* 22:559–570.

Burnashev, N., R. Schoepfer, H. Monyer, J.P. Ruppersberg, W. Gunther, P.H. Seeburg, and B. Sakmann. 1992. Control by asparagine residues of calcium permeability and magnesium blockade in the NMDA receptor. *Science.* 257:1415–1419.

Chen, G.Q., C.H. Cui, M.L. Mayer, and E. Gouaux. 1999. Functional characterization of a potassium-selective prokaryotic glutamate receptor. *Nature.* 402:817–821.

Doyle, D.A., J.H. Morais Cabral, R.A. Pfuetzner, A. Kuo, J.M. Glubis, S.L. Cohen, B.T. Chait, and R. MacKinnon. 1998. The structure of the potassium channel: molecular basis of conduction and selectivity. *Science.* 280:69–77.

Fayyazuddin, A., A. Villaroel, A. Le Goff, J. Lerma, and J. Neyton. 2000. Four residues of the extracellular N-terminal domain of the NR2A subunit control high-affinity Zn^{2+} binding to NMDA receptors. *Neuron.* 25:683–694.

Immke D, M. Wood, L. Kiss, and S.J. Korn. 1999. Potassium-dependent changes in the conformation of the Kv2.1 potassium channel pore. *J. Gen. Physiol.* 113:819–836.

Jiang, Y., and R. MacKinnon. 2000. The barium site in a potassium channel by X-ray crystallography. *J. Gen. Physiol.* 115:269–272.

Kuner, T., L.P. Wollmuth, A. Karlin, P.H. Seeburg, and B. Sakmann. 1996. Structure of the NMDA receptor channel M2 segment inferred from the accessibility of substituted cysteines. *Neuron.* 17: 343–352.

Kupper, J., P. Ascher, and J. Neyton. 1996. Probing the pore region of recombinant N-methyl-D-aspartate channels using external and internal magnesium block. *Proc. Natl. Acad. Sci. USA.* 93:8648–8653.

Mori, H., H. Masaki, T. Yamakura, and M. Mishina. 1992. Identification by mutagenesis of a Mg^{2+}-block site of the NMDA receptor channel. *Nature.* 358: 673–675.

Neyton, J., and C. Miller. 1988. Discrete Ba^{2+} block as a probe of ion occupancy and pore structure in the high conductance Ca^{2+}-activated K^+ channel. *J. Gen. Physiol.* 92:569–586.

Premkumar, L.S., and A. Auerbach. 1996. Identification of a high affinity divalent cation binding site near the entrance of the NMDA receptor channel. *Neuron.* 16:869–880.

Sharma, G., and C.F. Stevens. 1996a. A mutation that alters magnesium block of N-methyl-D-aspartate receptor channels. *Proc. Natl. Acad. Sci. USA.* 93:9259–9263.

Sharma, G., and C.F. Stevens. 1996b. Interactions between two divalent ion binding sites in N-methyl-D-aspartate receptor channels. *Proc. Natl. Acad. Sci. USA.* 93:14170–14175.

Williams, K., A.J. Pahk, K. Kashiwagi, T. Masuko, N.D. Nguyen, and K. Igarashi. 1998. The selectivity filter of the N-methyl-D-aspartate receptor: a tryptophan residue controls block and permeation of Mg^{2+}. *Mol. Pharm.* 52: 933–941.

Wollmuth, L.P., T. Kuner, and B. Sakmann. 1998. Adjacent asparagines in the NR2-subunit of the NMDA receptor channel control the voltage-dependent block by extracellular Mg^{2+}. *J. Physiol.* 506:13–32.

Wood, M.W., H.M.A. VanDongen, and A.M.J. Vandongen. 1995. Structural conservation of ion conduction pathways in K channels and glutamate receptors. *Proc. Natl. Acad. Sci. USA.* 92:4882–4886.

Zhu, Y., and A. Auerbach. 2001. Na^+ occupancy and Mg^{2+} block of the *N*-methyl-D-aspartate receptor channel. *J. Gen. Physiol.* 117:275–285.